electronic reprint

CRYSTALLOGRAPHIC COMMUNICATIONS

ISSN: 2056-9890
journals.iucr.org/e

4-(4-Acetyl-5-methyl-1*H*-1,2,3-triazol-1-yl)benzonitrile: crystal structure and Hirshfeld surface analysis

Julio Zukerman-Schpector, Cássio da S. Dias, Ricardo S. Schwab, Mukesh M. Jotani and Edward R. T. Tiekink

Acta Cryst. (2018). E**74**, 1195–1200

Acta Cryst E CRYSTALLOGRAPHIC COMMUNICATIONS

ISSN 2056-9890

4-(4-Acetyl-5-methyl-1*H*-1,2,3-triazol-1-yl)benzonitrile: crystal structure and Hirshfeld surface analysis

Julio Zukerman-Schpector,[a]* Cássio da S. Dias,[b] Ricardo S. Schwab,[b] Mukesh M. Jotani[c] and Edward R. T. Tiekink[d]‡

[a]Laboratório de Cristalografia, Esterodinâmica e Modelagem Molecular, Departamento de Química, Universidade Federal de São Carlos, 13565-905 São Carlos, SP, Brazil, [b]Departamento de Química, Universidade Federal de São Carlos, 13565-905 São Carlos, SP, Brazil, [c]Department of Physics, Bhavan's Sheth R. A. College of Science, Ahmedabad, Gujarat 380001, India, and [d]Research Centre for Crystalline Materials, School of Science and Technology, Sunway University, 47500 Bandar Sunway, Selangor Darul Ehsan, Malaysia. *Correspondence e-mail: julio@power.ufscar.br

Received 27 July 2018
Accepted 29 July 2018

Edited by W. T. A. Harrison, University of Aberdeen, Scotland

‡ Additional correspondence author, e-mail: edwardt@sunway.edu.my.

Keywords: crystal structure; 1,2,3-triazol-1-yl; nitrile; Hirshfeld surface analysis; NCI plots.

CCDC reference: 1859008

Supporting information: this article has supporting information at journals.iucr.org/e

The title compound, $C_{12}H_{10}N_4O$, comprises a central 1,2,3-triazole ring (r.m.s. deviation = 0.0030 Å) flanked by N-bound 4-cyanophenyl and C-bound acetyl groups, which make dihedral angles of 54.64 (5) and 6.8 (3)° with the five-membered ring, indicating a twisted molecule. In the crystal, the three-dimensional architecture is sustained by carbonyl-C=O···π(triazoyl), cyano-C≡N···π(triazoyl) (these interactions are shown to be attractive based on non-covalent interaction plots) and π–π stacking interactions [intercentroid separation = 3.9242 (9) Å]. An analysis of the Hirshfeld surface shows the important contributions made by H···H (35.9%) and N···H (26.2%) contacts to the overall surface, as well as notable contributions by O···H (9.9%), C···H (8.7%), C···C (7.3%) and C···N (7.2%) contacts.

1. Chemical context

The 1,2,3-triazoles comprise an interesting class of heterocyclic compounds, with diverse applications in biological and material chemistry (Struthers *et al.*, 2010; Bonandi *et al.*, 2017; Dheer *et al.*, 2017). In particular, 1,2,3-triazoles containing a carbonyl or carboxyl group in their structures have received considerable attention as they are found in a great number of biologically and pharmaceutically active molecules that exhibit a broad spectrum of properties (Shu *et al.*, 2009; Morzherin *et al.*, 2011; Cheng *et al.*, 2012; Gilchrist *et al.*, 2014). In this context, the organocatalytic cycloaddition reaction of organic azides with β-ketoesters, β-ketoamides, enones and allyl ketones has proven to be a powerful strategy for the synthesis of such class of compounds (John *et al.*, 2015; Lima *et al.*, 2015). Although much progress has been achieved, most of the available methodologies usually employ a homogenous catalyst, which can be difficult to recover. In view of environmental concerns, very recently, we reported for the first time, a heterogeneous strategy for the synthesis of 1,4,5-tris-substituted-1,2,3-triazoles through the 1,3-dipolar cycloaddition between aryl azides and active methylene compounds using CuO nanoparticles as catalyst in DMSO under microwave irradiation (Dias *et al.*, 2018). The title compound, (I), was prepared in this study and despite having been prepared by another route in a different study (Kamalraj *et al.*, 2008), no crystal structure is available. The availability of crystals in the latter study prompted the present structural analysis.

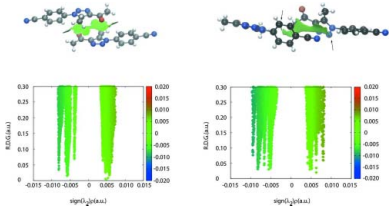

OPEN ACCESS

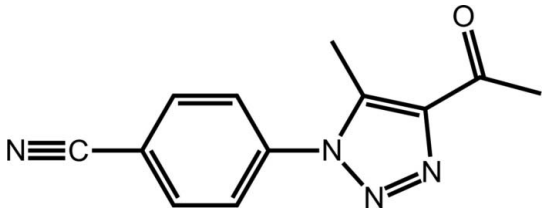

2. Structural commentary

The molecular structure of (I), Fig. 1, comprises an essentially planar 1,2,3-triazolyl ring with a r.m.s. deviation of the fitted atoms of 0.0030 Å; the maximum deviation of 0.0037 (9) Å is found for the N2 atom. A 4-cyanophenyl residue is connected to the 1,2,3-triazolyl ring at the N1-position and forms a dihedral angle of 54.64 (5)° with it, indicating a significant twist between the rings. By contrast, the acetyl group connected at the C2-position is approximately co-planar with the central ring, forming a dihedral angle of 6.8 (3)°. The dihedral angle between the phenyl and acetyl groups is 60.82 (13)°, indicating a dis-rotatory relationship. The acetyl-carbonyl group occupies a position approximately *syn* to the ring-bound methyl substituent with the C1—C2—C3—O1 and C4—C1—C2—C3 torsion angles being 6.2 (3) and −1.5 (3)°, respectively.

3. Supramolecular features

The molecular packing of (I) features interactions involving both the five- and six-membered rings. Centrosymmetrically related molecules are connected *via* carbonyl-C═O···π(triazoyl) interactions, Table 1. Further connections between molecules are of the type cyano-C≡N···π(triazoyl) to the opposite face of the five-membered ring (Fig. 2, Table 1), which together lead to a supramolecular layer parallel to ($\bar{1}$01). The O···π or N···π separations for these interactions are significantly longer that the van der Waals' separations for these species (3.32 and 3.35 Å, respectively) but the non-covalent interactions plots (see below) indicate that they are weakly attractive in nature. Connections between the layers giving rise to a three-dimensional architecture are weak π–π stacking interactions between centrosymmetrically related phenyl rings, with the inter-centroid separation being 3.9242 (9) Å; symmetry operation (i): 2 − *x*, 2 − *y*, 1 − *z*. A view of the unit cell contents is shown in Fig. 2. The specified and other weak intermolecular interactions are discussed in more detail below in *Hirshfeld surface analysis*.

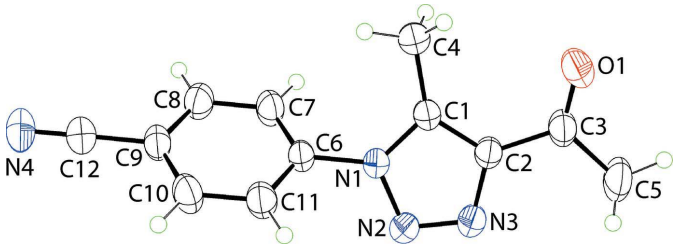

Figure 1
The molecular structure of (I), showing the atom-labelling scheme and displacement ellipsoids at the 50% probability level.

Table 1
π(Triazolyl) interaction geometry (Å, °).

*Cg*1 is the centroid of the N1–N3/C1/C2 ring.

D—H···*A*	*D*—H	H···*A*	*D*···*A*	*D*—H···*A*
C3—O1···*Cg*1^{i}	1.21 (1)	3.69 (1)	3.7359 (17)	83 (1)
C12—N4···*Cg*1^{ii}	1.14 (1)	3.68 (1)	3.8468 (19)	90 (1)

Symmetry codes: (i) $-x+1, -y+2, -z+1$; (ii) $x-\frac{1}{2}, -y+\frac{1}{2}, z-\frac{1}{2}$.

4. Hirshfeld surface analysis

The Hirshfeld surface calculations for (I) were performed in accord with related studies (Caracelli *et al.*, 2018) and provide information on the influence of other weak intermolecular interactions instrumental in the molecular packing. In addition to the presence of carbonyl-C═O···π(triazolyl) and cyano-C≡N···π(triazolyl) interactions (Table 1) in the formation of three-dimensional architecture as discussed above, the molecular packing also features weak C—H···N interactions. On the Hirshfeld surface mapped over d_{norm} in Fig. 3, these interactions are characterized as the bright-red spots near the

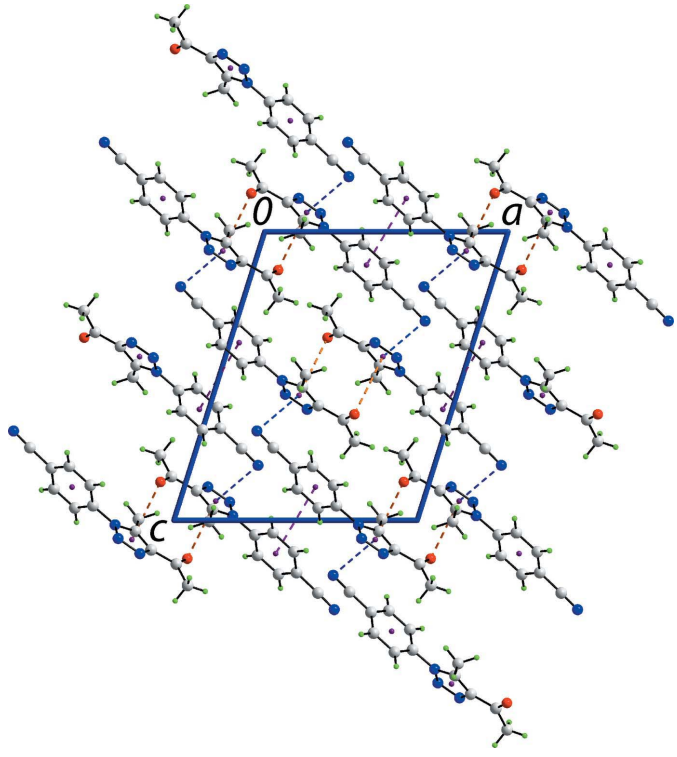

Figure 2
A view of the unit-cell contents shown in projection down the *b* axis. The C═ O···π(triazoyl), C≡N···π(triazoyl) and π(tolyl)–π(tolyl) contacts are shown as orange, blue and purple dashed lines, respectively.

Table 2
Summary of short interatomic contacts (Å) in (I).

Contact	Distance	Symmetry operation
H4*C*···H4*C*	2.39	$1-x, 1-y, 1-z$
H10···N3	2.48	$\frac{1}{2}+x, \frac{5}{2}-y, \frac{1}{2}+z$
H7···N4	2.58	$-\frac{1}{2}+x, \frac{3}{2}-y, -\frac{1}{2}+z$
H8···N4	2.53	$\frac{5}{2}-x, -\frac{1}{2}+y, \frac{3}{2}-z$
C4···O1	3.208 (2)	$1-x, 1-y, 1-z$

triazolyl-N3, cyano-N4 (Fig. 3*a*), phenyl-H8 and H10 atoms (Fig. 3*b*), and the diminutive-red spots near cyano-N4 (Fig. 3*b*) and phenyl-H7 (Fig. 3*a*) atoms. The influence of short interatomic C···O/O···C contacts involving methyl-C4 and carbonyl-O1 atoms (Table 2) is also observed as the faint-red spots near these atoms in Fig. 3*b*. The donors and acceptors of intermolecular C—H···N interactions are also evident as the blue and red regions corresponding to positive and negative electrostatic potentials, respectively, on the Hirshfeld surface

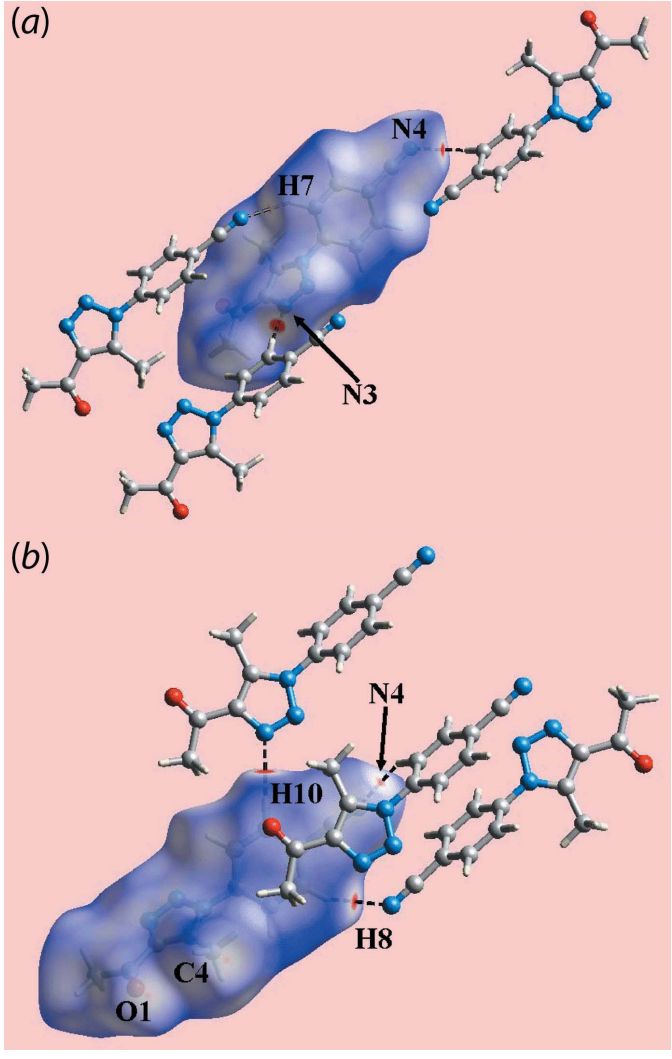

Figure 3
Two views of the Hirshfeld surface for (I) mapped over d_{norm} in the range −0.065 to +1.215 a.u.

Table 3
Percentage contributions of interatomic contacts to the Hirshfeld surface for (I).

Contact	Percentage contribution
H···H	35.9
N···H/H···N	26.2
O···H/H···O	9.9
C···H/H···C	8.7
C···C	7.3
C···N/N···C	7.2
N···N	2.1
C···O/O···C	1.4
N···O/O···N	1.4

mapped over electrostatic potential shown in Fig. 4. Views of the immediate environment about a reference molecule within the Hirshfeld surface mapped over the shape-index property, highlighting intermolecular C═O···π, C≡N···π and π–π stacking interactions, are illustrated in Fig. 5.

The overall two-dimensional fingerprint plot for (I) (Fig. 6*a*) and those delineated into H···H, N···H/H···N, O···H/H···O, C···H/H···C, C···C, C···N/N···C and N···N contacts (McKinnon *et al.*, 2007) are illustrated in Fig. 6*b*–*i*, respectively; the percentage contributions from identified interatomic contacts to the Hirshfeld surface are summarized in Table 3. The short interatomic H···H contact involving symmetry-related methyl-H4*C* atoms (Table 2) is viewed as the cone-shaped tip at $d_e + d_i \sim 2.3$ Å in the fingerprint plot delineated into H···H contacts (Fig. 6*b*). The second largest contribution to the Hirshfeld surface, *i.e.* 26.2%, is from N···H/H···N contacts (Fig. 6*c*) and arise from the intermolecular C—H···N contacts involving cyano-N4 and tria-

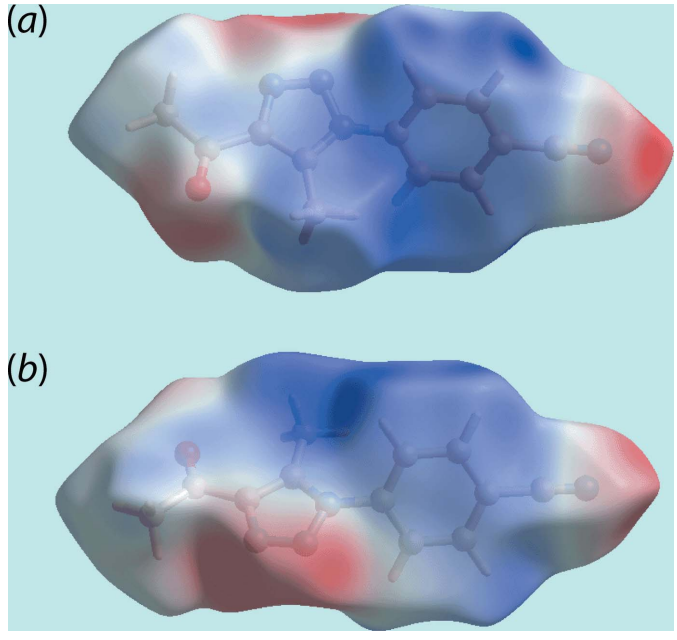

Figure 4
Two views of the Hirshfeld surface mapped over the electrostatic potential in the range −0.092 to +0.055 a.u. The red and blue regions represent negative and positive electrostatic potentials, respectively.

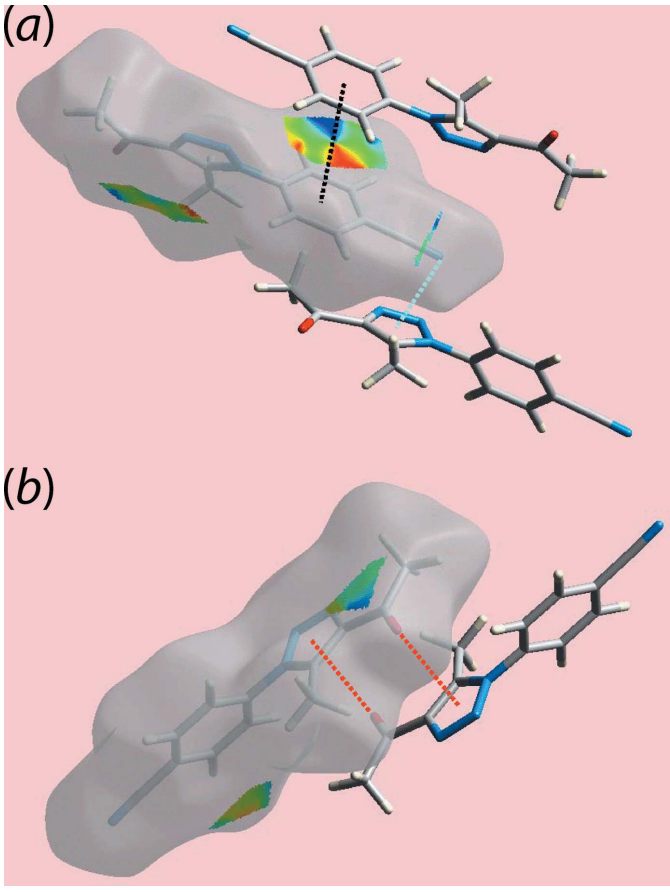

Figure 5
Views of the Hirshfeld surface mapped the shape-index property showing (*a*) π–π and C≡N···π interactions with black and sky-blue dotted lines, respectively and (*b*) C=O···π contacts with red-dotted lines.

zolyl-N3 atoms (Table 2) and are viewed as the pair of overlapping green and blue spikes with their tips at $d_e + d_i \sim 2.5$ Å. Although the carbonyl-O1 atom makes a significant contribution of 9.9% to the overall surface owing to interatomic O···H/H···O contacts, it is evident from the respective delineated fingerprint plot (Fig. 6*d*) that these are beyond van der Waals separations. The relatively small contribution from

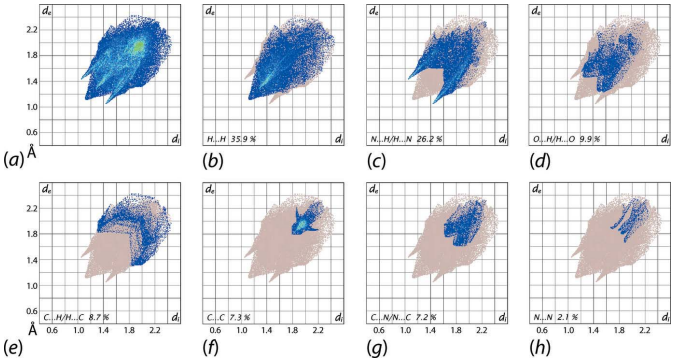

Figure 6
(*a*) The full two-dimensional fingerprint plot for (I) and (*b*)-(*h*) those delineated into H···H, N···H/H···N, O···H/H···O, C···H/H···C, C···C, C···N/N···C and N···N contacts, respectively.

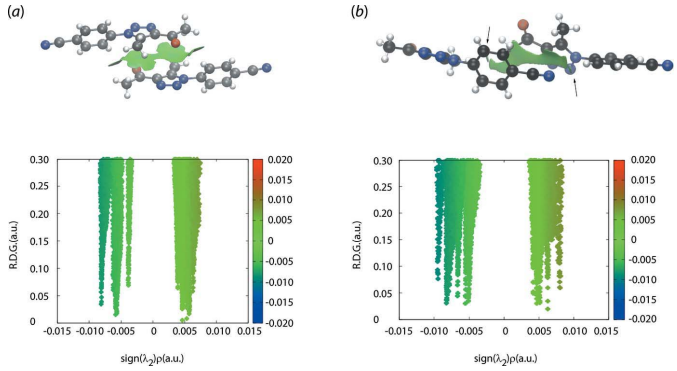

Figure 7
Non-covalent interaction plots for the (*a*) carbonyl-C= O···π(triazolyl) and (*b*) cyano-C≡N···π(triazolyl) interactions. The arrows in (*b*) indicate attractive phenyl-C—H···N(cyano) interactions (see text).

C···H/H···C contacts to the Hirshfeld surface (Table 3) is indicative of the absence of C—H···π contacts in the molecular packing, Fig. 6*e*. The weak π–π stacking interactions between symmetry related phenyl-(C6–C11) rings are evident from the fingerprint delineated into C···C contacts (Fig. 6*f*) as the rocket-like tip at $d_e + d_i \sim 3.6$ Å. The involvement of the triazolyl ring in intermolecular triazolyl-C≡N···π and carbonyl C=O···π contacts in the crystal is reflected from the percentage contributions due to C···N/N···C, C···O/O···C, N···N and N···O/O···N contacts to the Hirshfeld surface (Table 3). These intermolecular interactions are also evident from the fingerprint plots delineated into C···N/N···C, C···O/O···C and N···N contacts in Fig. 6*f*–*h*, respectively.

5. Non-covalent interaction plots

Non-covalent interaction (NCI) plots are a convenient means by which the nature of an interaction between residues may be assessed in terms of being attractive or otherwise (Johnson *et al.*, 2010; Contreras-García *et al.*, 2011). In NCI plots, a weakly attractive interaction will appear green on the isosurface, whereas attractive and repulsive interactions will result in blue and red isosurfaces, respectively. The NCI plots for the interacting entities of the carbonyl-C=O···π(triazolyl) and cyano-C≡N···π(triazolyl) interactions are shown in Fig. 7*a*,*b*, indicating the weakly attractive nature of these interactions. The arrows in Fig. 7*b*, highlight a weak phenyl-C—H···N(cyano) interaction (Table 2).

6. Database survey

There are four closely related compounds in the literature whereby the cyano group of (I) is replaced by chloride and bromide, which are isostructural (Zeghada *et al.*, 2011), methyl (El-Hiti *et al.*, 2017) and nitro (Vinutha *et al.* (2013); two independent molecules comprise the asymmetric unit of the nitro compound. Key dihedral angle data are included in Table 4. This shows that the greatest variations in dihedral angles between the phenyl and acetyl residues is found for the two independent molecules of the nitro compound. The

Table 4
Dihedral angle data (°) for (I) and 4-*X*-phenyl derivatives.

X	triazolyl/phenyl	triazolyl/acetyl	phenyl/acetyl	Ref.
Me	50.11 (7)	6.12 (18)	50.14 (12)	El-Hiti *et al.* (2017)
Cl	45.60 (4)	6.97 (9)	45.19 (6)	Zeghada *et al.* (2011)
Br	47.03 (5)	7.08 (12)	46.5 (7)	Zeghada *et al.* (2011)
NO_2[a]	38.26 (15)	13.4 (4)	27.9 (3)	Vinutha *et al.* (2013)
	87.11 (18)	15.2 (3)	74.4 (2)	
C≡N	54.64 (5)	6.8 (3)	60.82 (13)	This work

Note: (*a*) Two independent molecules comprise the asymmetric unit.

different relative conformations in the aforementioned molecules is highlighted in the overlay diagram of Fig. 8.

7. Synthesis and crystallization

Compound (I) was prepared as described in the literature (Dias *et al.*, 2018) and crystals were obtained by the slow evaporation from its ethyl acetate/hexane (*v*/*v*) solution. M.p. 426–428 K. ^{1}H NMR (400 MHz, $CDCl_3$) δ = 7.91 (*d*, *J* = 8.7 Hz, 2H), 7.65 (*d*, *J* = 8.7 Hz, 2H), 2.76 (*s*, 3H), 2.66 (*s*, 3H). ^{13}C NMR (100 MHz,$CDCl_3$) δ = 194.30, 144.20, 138.89, 137.42, 133.85, 125.84, 117.51, 114.23, 28.10, 10.43 ppm.

8. Refinement details

Crystal data, data collection and structure refinement details are summarized in Table 5. The carbon-bound H atoms were placed in calculated positions (C—H = 0.93–0.96 Å) and were included in the refinement in the riding model approximation, with U_{iso}(H) set to 1.2–1.5U_{eq}(C).

Acknowledgements

The Brazilian agencies Coordination for the Improvement of Higher Education Personnel, CAPES, National Council for Scientific and Technological Development, CNPq, for a scholarship to JZ-S (303207/2017–5) are acknowledged for support. Funding for this research was provided by the National Council for Scientific and Technological Development, CNPq, (awards No. 303207/2017–5; 475203/2013–5), São Paulo Research Foundation-FAPESP (2013/06558–3) and GlaxoSmithKline-FAPESP (2014/50249–8). We thank Professor Regina H. A. Santos from IQSC-USP for the X-ray data collection.

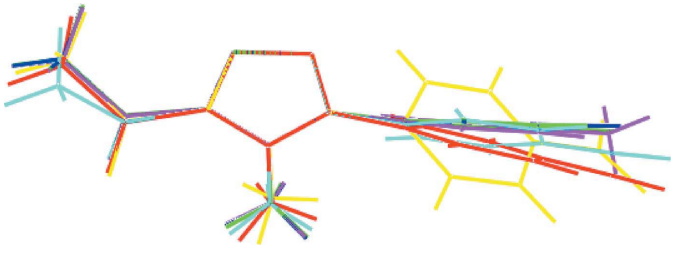

Figure 8
Overlay diagram for (I) and 4-*X*-phenyl derivatives: (I) (red image), *X* = Cl (green), *X* = Br (blue), *X* = Me (pink), *X* = NO_2 (first independent molecule; aqua) and *X* = NO_2 (second molecule; yellow). The molecules have been overlapped so that the triazolyl rings are coincident.

Table 5
Experimental details.

Crystal data	
Chemical formula	$C_{12}H_{10}N_4O$
M_r	226.24
Crystal system, space group	Monoclinic, $P2_1/n$
Temperature (K)	293
a, *b*, *c* (Å)	11.8533 (5), 6.8299 (3), 14.7329 (6)
β (°)	107.477 (1)
V (Å^3)	1137.67 (8)
Z	4
Radiation type	Mo *K*α
μ (mm^{-1})	0.09
Crystal size (mm)	0.44 × 0.27 × 0.12
Data collection	
Diffractometer	Bruker APEXII CCD
Absorption correction	Multi-scan (*SADABS*; Sheldrick, 1996)
T_{min}, T_{max}	0.726, 0.745
No. of measured, independent and observed [$I > 2\sigma(I)$] reflections	30812, 2333, 2083
R_{int}	0.023
(sin $\theta/\lambda)_{max}$ (Å^{-1})	0.625
Refinement	
$R[F^2 > 2\sigma(F^2)]$, $wR(F^2)$, *S*	0.044, 0.126, 1.10
No. of reflections	2333
No. of parameters	156
H-atom treatment	H-atom parameters constrained
$\Delta\rho_{max}$, $\Delta\rho_{min}$ (e Å^{-3})	0.21, −0.20

Computer programs: *APEX2* and *SAINT* (Bruker, 2009), *SIR2014* (Burla *et al.*, 2015), *SHELXL2014* (Sheldrick, 2015), *ORTEP-3 for Windows* (Farrugia, 2012), *DIAMOND* (Brandenburg, 2006), *MarvinSketch* (ChemAxon, 2010) and *publCIF* (Westrip, 2010).

Funding information

Funding for this research was provided by: National Council for Scientific and Technological Development, CNPq (grant No. 303207/2017–5); National Council for Scientific and Technological Development, CNPq (grant No. 475203/2013–5); São Paulo Research Foundation-FAPESP (grant No. 2013/06558-3); GlaxoSmithKline-FAPESP (grant No. 2014/50249-8).

References

Bonandi, E., Christodoulou, M. S., Fumagalli, G., Perdicchia, D., Rastelli, G. & Passarella, D. (2017). *Drug Discov. Today*, **22**, 1572–1581.
Brandenburg, K. (2006). *DIAMOND*. Crystal Impact GbR, Bonn, Germany.
Bruker (2009). *APEX2* and *SAINT*. Bruker AXS Inc., Madison, Wisconsin, USA.
Burla, M. C., Caliandro, R., Carrozzini, B., Cascarano, G. L., Cuocci, C., Giacovazzo, C., Mallamo, M., Mazzone, A. & Polidori, G. (2015). *J. Appl. Cryst.* **48**, 306–309.
Caracelli, I., Zukerman-Schpector, J., Traesel, H. J., Olivato, P. R., Jotani, M. M. & Tiekink, E. R. T. (2018). *Acta Cryst.* E**74**, 703–708.
ChemAxon (2010). *Marvinsketch*. http://www.chemaxon.com.
Cheng, H., Wan, J., Lin, M.-I., Liu, Y., Lu, X., Liu, J., Xu, Y., Chen, J., Tu, Z., Cheng, Y.-S. E. & Ding, K. (2012). *J. Med. Chem.* **55**, 2144–2153.

Contreras-García, J., Johnson, E. R., Keinan, S., Chaudret, R., Piquemal, J.-P., Beratan, D. N. & Yang, W. (2011). *J. Chem. Theory Comput.* **7**, 625–632.
Dheer, D., Singh, V. & Shankar, R. (2017). *Bioorg. Chem.* **71**, 30–54.
Dias, C. da S., Lima, T. de M., Lima, C. G. S., Zukerman-Schpector, J. & Schwab, R. S. (2018). *ChemistrySelect*, **3**, 6195–6202.
El-Hiti, G. A., Abdel-Wahab, B. F., Alotaibi, M. H., Hegazy, A. S. & Kariuki, B. M. (2017). *IUCrData*, x171782.
Farrugia, L. J. (2012). *J. Appl. Cryst.* **45**, 849–854.
Gilchrist, J., Dutton, S., Diaz-Bustamante, M., McPherson, A., Olivares, N., Kalia, J., Escayg, A. & Bosmans, F. (2014). *Chem. Biol.* **9**, 1204–1212.
John, J., Thomas, J. & Dehaen, W. (2015). *Chem. Commun.* **51**, 10797–10806.
Johnson, E. R., Keinan, S., Mori-Sánchez, P., Contreras-García, J., Cohen, A. J. & Yang, W. (2010). *J. Am. Chem. Soc.* **132**, 6498–6506.
Kamalraj, V. R., Senthil, S. & Kannan, P. (2008). *J. Mol. Struct.* **892**, 210–215.
Lima, C. G. S., Ali, A., van Berkel, S. S., Westermann, B. & Paixão, M. W. (2015). *Chem. Commun.* **51**, 10784–10796.
McKinnon, J. J., Jayatilaka, D. & Spackman, M. A. (2007). *Chem. Commun.* pp. 3814–3816.
Morzherin, Y., Prokhorova, P. E., Musikhin, D. A., Glukhareva, T. V. & Fan, Z. (2011). *Pure Appl. Chem.* **83**, 715–722.
Sheldrick, G. M. (1996). *SADABS*. University of Göttingen, Germany.
Sheldrick, G. M. (2015). *Acta Cryst.* C**71**, 3–8.
Shu, H., Izenwasser, S., Wade, D., Stevens, E. D. & Trudell, M. L. (2009). *Bioorg. Med. Chem. Lett.* **19**, 891–893.
Struthers, H., Mindt, T. L. & Schibli, R. (2010). *Dalton Trans.* **39**, 675–696.
Vinutha, N., Madan Kumar, S., Nithinchandra, Balakrishna, K., Lokanath, N. K. & Revannasiddaiah, D. (2013). *Acta Cryst.* E**69**, o1724.
Westrip, S. P. (2010). *J. Appl. Cryst.* **43**, 920–925.
Zeghada, S., Bentabed-Ababsa, G., Derdour, A., Abdelmounim, S., Domingo, L. R., Sáez, J. A., Roisnel, T., Nassar, E. & Mongin, F. (2011). *Org. Biomol. Chem.* **9**, 4295–4305.

supporting information

Acta Cryst. (2018). E**74**, 1195-1200 [https://doi.org/10.1107/S2056989018010885]

4-(4-Acetyl-5-methyl-1*H*-1,2,3-triazol-1-yl)benzonitrile: crystal structure and Hirshfeld surface analysis

Julio Zukerman-Schpector, Cássio da S. Dias, Ricardo S. Schwab, Mukesh M. Jotani and Edward R. T. Tiekink

Computing details

Data collection: *APEX2* (Bruker, 2009); cell refinement: *SAINT* (Bruker, 2009); data reduction: *SAINT* (Bruker, 2009); program(s) used to solve structure: *SIR2014* (Burla *et al.*, 2015); program(s) used to refine structure: *SHELXL2014* (Sheldrick, 2015); molecular graphics: *ORTEP-3 for Windows* (Farrugia, 2012) and *DIAMOND* (Brandenburg, 2006); software used to prepare material for publication: *MarvinSketch* (ChemAxon, 2010) and *publCIF* (Westrip, 2010).

4-(4-Acetyl-5-methyl-1*H*-1,2,3-triazol-1-yl)benzonitrile

Crystal data

$C_{12}H_{10}N_4O$
$M_r = 226.24$
Monoclinic, $P2_1/n$
$a = 11.8533$ (5) Å
$b = 6.8299$ (3) Å
$c = 14.7329$ (6) Å
$\beta = 107.477$ (1)°
$V = 1137.67$ (8) Å^3
$Z = 4$
$F(000) = 472$
$D_x = 1.321$ Mg m^{-3}
Mo $K\alpha$ radiation, $\lambda = 0.71073$ Å
Cell parameters from 9978 reflections
$\theta = 2.6$–$26.3°$
$\mu = 0.09$ mm^{-1}
$T = 293$ K
Irregular, colourless
0.44 × 0.27 × 0.12 mm

Data collection

Bruker APEXII CCD diffractometer
φ and ω scans
Absorption correction: multi-scan (SADABS; Sheldrick, 1996)
$T_{min} = 0.726$, $T_{max} = 0.745$
30812 measured reflections
2333 independent reflections
2083 reflections with $I > 2\sigma(I)$
$R_{int} = 0.023$
$\theta_{max} = 26.4°$, $\theta_{min} = 1.9°$
$h = -14 \rightarrow 14$
$k = -8 \rightarrow 8$
$l = -18 \rightarrow 18$

Refinement

Refinement on F^2
Least-squares matrix: full
$R[F^2 > 2\sigma(F^2)] = 0.044$
$wR(F^2) = 0.126$
$S = 1.10$
2333 reflections
156 parameters
0 restraints
Primary atom site location: structure-invariant direct methods
Hydrogen site location: inferred from neighbouring sites
H-atom parameters constrained
$w = 1/[\sigma^2(F_o^2) + (0.0573P)^2 + 0.3916P]$ where $P = (F_o^2 + 2F_c^2)/3$
$(\Delta/\sigma)_{max} < 0.001$

$\Delta\rho_{max}$ = 0.21 e Å^{-3} $\Delta\rho_{min}$ = −0.20 e Å^{-3}

Special details

Geometry. All esds (except the esd in the dihedral angle between two l.s. planes) are estimated using the full covariance matrix. The cell esds are taken into account individually in the estimation of esds in distances, angles and torsion angles; correlations between esds in cell parameters are only used when they are defined by crystal symmetry. An approximate (isotropic) treatment of cell esds is used for estimating esds involving l.s. planes.

Fractional atomic coordinates and isotropic or equivalent isotropic displacement parameters (Å^2)

	x	*y*	*z*	U_{iso}*/U_{eq}
O1	0.39515 (11)	0.7197 (2)	0.36712 (11)	0.0785 (5)
N1	0.73587 (10)	0.95924 (17)	0.48424 (8)	0.0357 (3)
N2	0.70535 (11)	1.13354 (19)	0.43684 (10)	0.0476 (3)
N3	0.59641 (11)	1.11608 (19)	0.38456 (10)	0.0462 (3)
N4	1.27442 (13)	0.8725 (3)	0.80947 (11)	0.0623 (4)
C1	0.64418 (11)	0.8326 (2)	0.46207 (10)	0.0364 (3)
C2	0.55549 (12)	0.9350 (2)	0.39775 (10)	0.0364 (3)
C3	0.43345 (13)	0.8728 (2)	0.34833 (11)	0.0451 (4)
C4	0.64687 (15)	0.6346 (3)	0.50374 (14)	0.0614 (5)
H4A	0.7168	0.6210	0.5570	0.092*
H4B	0.6473	0.5378	0.4566	0.092*
H4C	0.5782	0.6168	0.5246	0.092*
C5	0.35961 (15)	1.0069 (3)	0.27426 (14)	0.0668 (6)
H5A	0.3902	1.0108	0.2209	0.100*
H5B	0.3615	1.1361	0.3004	0.100*
H5C	0.2795	0.9602	0.2538	0.100*
C6	0.85161 (11)	0.9389 (2)	0.55064 (9)	0.0354 (3)
C7	0.92321 (13)	0.7849 (2)	0.54291 (11)	0.0454 (4)
H7	0.8976	0.6944	0.4938	0.054*
C8	1.03376 (14)	0.7662 (2)	0.60904 (11)	0.0482 (4)
H8	1.0827	0.6622	0.6050	0.058*
C9	1.07120 (12)	0.9032 (2)	0.68124 (10)	0.0403 (3)
C10	0.99970 (13)	1.0600 (3)	0.68695 (11)	0.0494 (4)
H10	1.0261	1.1532	0.7347	0.059*
C11	0.88901 (13)	1.0776 (2)	0.62138 (11)	0.0472 (4)
H11	0.8401	1.1820	0.6249	0.057*
C12	1.18561 (13)	0.8846 (3)	0.75178 (11)	0.0470 (4)

Atomic displacement parameters (Å^2)

	U^{11}	U^{22}	U^{33}	U^{12}	U^{13}	U^{23}
O1	0.0477 (7)	0.0734 (9)	0.0927 (10)	−0.0232 (7)	−0.0117 (7)	0.0290 (8)
N1	0.0288 (6)	0.0351 (6)	0.0380 (6)	−0.0012 (4)	0.0023 (5)	0.0037 (5)
N2	0.0366 (6)	0.0393 (7)	0.0589 (8)	−0.0023 (5)	0.0022 (6)	0.0124 (6)
N3	0.0334 (6)	0.0443 (7)	0.0534 (7)	0.0003 (5)	0.0020 (5)	0.0125 (6)
N4	0.0443 (8)	0.0714 (11)	0.0552 (9)	0.0006 (7)	−0.0094 (7)	−0.0012 (7)
C1	0.0307 (6)	0.0376 (7)	0.0364 (7)	−0.0032 (5)	0.0036 (5)	0.0021 (6)
C2	0.0302 (7)	0.0401 (7)	0.0361 (7)	−0.0003 (5)	0.0054 (5)	0.0049 (6)

C3	0.0317 (7)	0.0553 (9)	0.0424 (8)	−0.0039 (6)	0.0024 (6)	0.0068 (7)
C4	0.0469 (9)	0.0476 (10)	0.0732 (12)	−0.0105 (7)	−0.0071 (8)	0.0224 (8)
C5	0.0377 (8)	0.0836 (14)	0.0641 (11)	−0.0017 (9)	−0.0074 (8)	0.0234 (10)
C6	0.0273 (6)	0.0391 (7)	0.0358 (7)	−0.0026 (5)	0.0033 (5)	0.0015 (6)
C7	0.0376 (8)	0.0462 (8)	0.0436 (8)	0.0026 (6)	−0.0009 (6)	−0.0114 (6)
C8	0.0383 (8)	0.0475 (9)	0.0512 (9)	0.0077 (6)	0.0019 (7)	−0.0067 (7)
C9	0.0301 (7)	0.0493 (8)	0.0365 (7)	−0.0029 (6)	0.0025 (5)	0.0008 (6)
C10	0.0388 (8)	0.0544 (9)	0.0477 (8)	−0.0026 (7)	0.0018 (7)	−0.0157 (7)
C11	0.0356 (8)	0.0460 (8)	0.0538 (9)	0.0032 (6)	0.0038 (7)	−0.0120 (7)
C12	0.0385 (8)	0.0526 (9)	0.0434 (8)	−0.0017 (7)	0.0025 (7)	−0.0012 (7)

Geometric parameters (Å, º)

O1—C3	1.205 (2)	C5—H5A	0.9600
N1—C1	1.3500 (17)	C5—H5B	0.9600
N1—N2	1.3726 (17)	C5—H5C	0.9600
N1—C6	1.4326 (16)	C6—C7	1.378 (2)
N2—N3	1.2952 (17)	C6—C11	1.379 (2)
N3—C2	1.3634 (19)	C7—C8	1.384 (2)
N4—C12	1.140 (2)	C7—H7	0.9300
C1—C2	1.3762 (19)	C8—C9	1.385 (2)
C1—C4	1.482 (2)	C8—H8	0.9300
C2—C3	1.4734 (19)	C9—C10	1.384 (2)
C3—C5	1.491 (2)	C9—C12	1.4452 (19)
C4—H4A	0.9600	C10—C11	1.381 (2)
C4—H4B	0.9600	C10—H10	0.9300
C4—H4C	0.9600	C11—H11	0.9300
C1—N1—N2	111.26 (11)	C3—C5—H5C	109.5
C1—N1—C6	129.75 (12)	H5A—C5—H5C	109.5
N2—N1—C6	118.91 (11)	H5B—C5—H5C	109.5
N3—N2—N1	106.62 (11)	C7—C6—C11	121.37 (13)
N2—N3—C2	109.42 (12)	C7—C6—N1	120.33 (12)
N1—C1—C2	103.53 (12)	C11—C6—N1	118.29 (13)
N1—C1—C4	124.68 (12)	C6—C7—C8	119.25 (14)
C2—C1—C4	131.77 (13)	C6—C7—H7	120.4
N3—C2—C1	109.16 (12)	C8—C7—H7	120.4
N3—C2—C3	121.99 (13)	C7—C8—C9	119.71 (14)
C1—C2—C3	128.84 (14)	C7—C8—H8	120.1
O1—C3—C2	121.25 (14)	C9—C8—H8	120.1
O1—C3—C5	121.51 (15)	C10—C9—C8	120.56 (13)
C2—C3—C5	117.25 (14)	C10—C9—C12	118.92 (14)
C1—C4—H4A	109.5	C8—C9—C12	120.52 (14)
C1—C4—H4B	109.5	C11—C10—C9	119.66 (14)
H4A—C4—H4B	109.5	C11—C10—H10	120.2
C1—C4—H4C	109.5	C9—C10—H10	120.2
H4A—C4—H4C	109.5	C6—C11—C10	119.42 (14)
H4B—C4—H4C	109.5	C6—C11—H11	120.3

C3—C5—H5A	109.5	C10—C11—H11	120.3
C3—C5—H5B	109.5	N4—C12—C9	177.85 (18)
H5A—C5—H5B	109.5		

C1—N1—N2—N3	−0.81 (17)	C1—C2—C3—C5	−173.75 (16)
C6—N1—N2—N3	−177.77 (12)	C1—N1—C6—C7	57.1 (2)
N1—N2—N3—C2	0.54 (17)	N2—N1—C6—C7	−126.64 (15)
N2—N1—C1—C2	0.72 (16)	C1—N1—C6—C11	−123.36 (17)
C6—N1—C1—C2	177.26 (13)	N2—N1—C6—C11	52.95 (19)
N2—N1—C1—C4	−177.72 (16)	C11—C6—C7—C8	1.7 (2)
C6—N1—C1—C4	−1.2 (2)	N1—C6—C7—C8	−178.73 (14)
N2—N3—C2—C1	−0.10 (18)	C6—C7—C8—C9	−0.6 (3)
N2—N3—C2—C3	179.34 (14)	C7—C8—C9—C10	−1.0 (3)
N1—C1—C2—N3	−0.38 (16)	C7—C8—C9—C12	179.08 (15)
C4—C1—C2—N3	177.90 (17)	C8—C9—C10—C11	1.5 (3)
N1—C1—C2—C3	−179.78 (14)	C12—C9—C10—C11	−178.55 (15)
C4—C1—C2—C3	−1.5 (3)	C7—C6—C11—C10	−1.2 (2)
N3—C2—C3—O1	−173.09 (17)	N1—C6—C11—C10	179.25 (14)
C1—C2—C3—O1	6.2 (3)	C9—C10—C11—C6	−0.4 (3)
N3—C2—C3—C5	6.9 (2)		

Hydrogen-bond geometry (Å, º)

π(Triazolyl) interaction geometry (Å, °) for (I). Cg1 is the centroid of the N1–N3/C1/C2 ring.

D—H···*A*	*D*—H	H···*A*	*D*···*A*	*D*—H···*A*
C3—O1···*Cg*1^{i}	1.21 (1)	3.69 (1)	3.7359 (17)	83 (1)
C12—N4···*Cg*1^{ii}	1.14 (1)	3.68 (1)	3.8468 (19)	90 (1)

Symmetry codes: (i) −*x*+1, −*y*+2, −*z*+1; (ii) *x*−1/2, −*y*+1/2, *z*−1/2.